A&A 401, 959–974 (2003)
DOI: 10.1051/0004-6361:20030188

Astronomy & Astrophysics

New neighbours

V. 35 DENIS late-M dwarfs between 10 and 30 parsecs

N. Phan-Bao[1,2], F. Crifo[2], X. Delfosse[3], T. Forveille[3,4], J. Guibert[1,2], J. Borsenberger[5], N. Epchtein[6], P. Fouqué[7,8], G. Simon[2], and J. Vetois[1,9]

[1] Centre d'Analyse des Images, GEPI, Observatoire de Paris, 61 avenue de l'Observatoire, 75014 Paris, France
[2] GEPI, Observatoire de Paris, 5 place J. Janssen, 92195 Meudon Cedex, France
[3] Laboratoire d'Astrophysique de Grenoble, Université J. Fourier, BP 53, 38041 Grenoble, France
[4] Canada-France-Hawaii Telescope Corporation, 65-1238 Mamalahoa Highway, Kamuela, HI 96743, USA
[5] SIO, Observatoire de Paris, 5 place J. Janssen, 92195 Meudon Cedex, France
[6] Observatoire de la Côte d'Azur, Département Fresnel, BP 4229, 06304 Nice Cedex 4, France
[7] LESIA, Observatoire de Paris, 5 place J. Janssen, 92195 Meudon Cedex, France
[8] European Southern Observatory, Casilla 19001, Santiago 19, Chile
[9] École Normale Supérieure de Cachan, 61 avenue du Président-Wilson, 94230 Cachan, France

Received 15 July 2002 / Accepted 31 January 2003

Abstract. This paper reports updated results on our systematic mining of the DENIS database for nearby very cool M-dwarfs (M 6V-M 8V, $2.0 \leq I - J \leq 3.0$, photometric distance within 30 pc), initiated by Phan-Bao et al. (2001, hereafter Paper I). We use M dwarfs with well measured parallaxes (HIP, GCTP, ...) to calibrate the DENIS (M_I, $I - J$) colour-luminosity relationship. The resulting distance error for single dwarfs is about 25%. Proper motions, as well as B and R magnitudes, were measured on archive Schmidt plates for those stars in the DENIS database that meet the photometric selection criteria. We then eliminate the giants by a Reduced Proper Motion cutoff, which is significantly more selective than a simple proper motion cutoff. It greatly reduces the selection bias against low tangential velocity stars, and results in a nearly complete sample. Here we present new data for 62 red dwarf candidates selected over 5700 square degrees in the DENIS database. 26 of those originate in the 2100 square degrees analysed in Paper I, with improved parameters here, and 36 were found in 3600 additional square degrees. 25 of those are new nearby dwarfs. We determine from that sample of 62 stars a stellar density for $12.0 \leq M_I \leq 14.0$ of $\overline{\Phi}_{I\ \mathrm{cor}} = (2.2 \pm 0.4) \times 10^{-3}$ stars pc^{-3} mag^{-1}. This value is consistent with photometric luminosity functions measured from deeper and smaller-field observations, but not with the nearby star luminosity function. In addition we cross-identified the NLTT and DENIS catalogues to find 15 similar stars, in parts of the sky not yet covered by the colour-selected search. We present distance and luminosity estimates for these 15 stars, 10 of which are newly recognized nearby dwarfs. A similar search in Paper I produced 4 red dwarf candidates, and we have thus up to now identified a total of 35 new nearby late-M dwarfs.

Key words. astrometry – stars: low mass, brown dwarfs – solar neighbourhood

1. Introduction

The stellar content of the solar neighbourhood is once again a very active research field, revived in large part by the vast amounts of new data from the near-Infrared surveys DENIS (Epchtein 1997) and 2MASS (Skrutskie et al. 1997) and the optical Sloan Digital Sky Survey (York et al. 2000; Hawley et al. 2002). These surveys have identified much fainter and cooler objects, and required the extension of the spectral classification system by two new spectral classes, the L and T dwarfs (Martín et al. 1997; Kirkpatrick et al. 1999). As expected, the surveys also detect large numbers of less extreme late-M dwarfs. As shown by Gliese et al. (1986) the census of the solar neighbourhood is rather incomplete for late M dwarfs, and their actual number density is not very well established.

In Paper I (Phan-Bao et al. 2001), we presented 30 nearby ($d_{\mathrm{phot}} < 30$ pc) late-M dwarfs ($2.0 \leq I - J \leq 3.0$, M 6–M 8) with high proper motions: 26, a few of which were previously known from other sources, were photometrically selected from 2100 square degrees of DENIS data, and 4 were identified by cross-identifying the LHS (Luyten 1979) and DENIS catalogues over a larger sky area. Here we repeat the analysis of Paper I with an improved ($I - J$, M_I) relation, calibrated specifically for the DENIS filter set, and extend the colour selection to a further 3600 square degrees. We also use an improved dwarf/giant discrimination criterion, based

Send offprint requests to: F. Crifo,
e-mail: francoise.crifo@obspm.fr

on the reduced proper motion rather than the simple proper motion cutoff which is commonly used for that purpose (e.g. Scholz et al. 2001; and Paper I). This allows us to dig down to significantly lower proper motions, and thus to identify additional dwarf candidates. Finally, we systematically search the DENIS database for southern NLTT stars (Luyten 1980) that have colours in the same ($2 \leq I - J \leq 3.0$) range.

Section 2 presents the DENIS colour-magnitude relation, and Sect. 3 reviews the sample selection. Section 4 discusses the proper motion measurements and the calibration of the B and R photographic photometry. Section 5 presents the giant/dwarf discrimination from Reduced Proper Motion plots, and Sect. 7 a rough estimation of effective temperatures. We discuss the completeness of the sample in Sect. 6 and indicate future directions in Sect. 8.

2. DENIS colour-magnitude relation

The DEep Near Infrared Survey (DENIS) (Epchtein 1997) systematically surveyed the southern sky in two near-infrared (J and K_S) and one optical (I) band. Its extensive sky coverage, broad wavelength baseline, and moderately deep exposures (I = 18.5, J = 16, K_S = 13.5) make it a very efficient tool at identifying faint and cool nearby stars.

In Paper I, we estimated distances to potential DENIS red dwarfs using the Cousins-CIT ($I_C - J_{CIT}$, M_I) relation for M dwarfs of Delfosse (1997b). We also noted that for red stars the DENIS photometric system and the standard Cousins-CIT system differ by ~0.1 mag for the K band, but by less than 0.05 mag for the I and J bands (Delfosse 1997b). The Delfosse (1997b) $I - J$ relation therefore applies reasonably well to DENIS photometry, but with progress in the DENIS data reduction it has now become possible, and preferable, to directly calibrate a DENIS colour-magnitude relation. Of the three colours that can be formed from DENIS photometry, $J - K$ is a very poor spectral type diagnostic for M dwarfs, while $I - J$ and $I - K$ are both excellent. From a practical point of view, DENIS is significantly more sensitive to M dwarfs at J than at K. We therefore chose to calibrate the ($I - J$, M_I) relation.

We searched the following trigonometric parallax catalogues for reference M dwarfs with a DENIS counterpart fainter than the I saturation limit of I = 9 and with $I - J > 1.0$:

- the Hipparcos catalogue (ESA 1997) for 63 relatively bright stars. As the limiting magnitude of the HIP catalogue is $V \sim 12.0$, it contains few very red dwarfs;
- the GCTP catalogue (van Altena et al. 1995) for 29 mostly fainter stars;
- 6 faint stars from Tinney et al. (1995), Tinney (1996); one from Henry et al. (1997) and one late M dwarf from Deacon & Hambly (2001).

We excluded known doubles as well as large amplitude variables, but had to accept a number of low amplitude flare stars, with peak visible light amplitude of 0.1 to 0.3 mag.

We did not correct the resulting absolute magnitudes for the Lutz-Kelker bias, since the complex selection pedigree of our sample makes a quantitative analysis of that bias almost impossible. Arenou & Luri (1999) conclude that it is preferable to apply no correction in such cases. The errors on the parallaxes are fortunately small, so that neglecting that correction does not appreciably contribute to the overall errors.

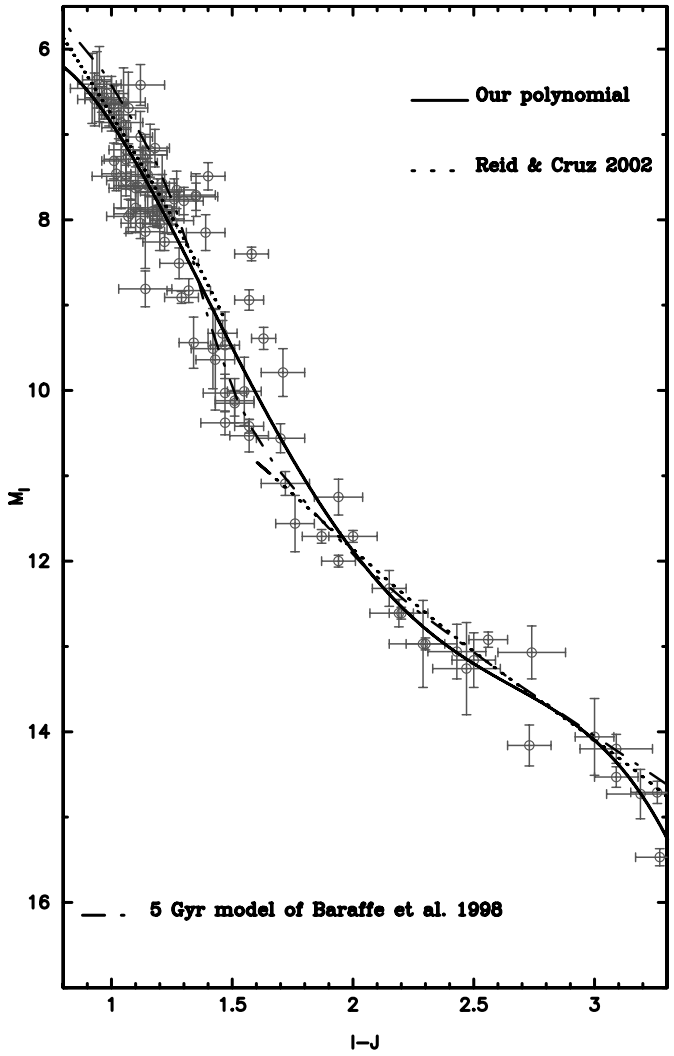

Fig. 1. ($M_I, I - J$) HR diagram for single M dwarfs with known trigonometric parallaxes (data in Table 1).

Figure 1 shows the resulting ($I - J$, M_I) plot, and the corresponding 4th order polynomial fit:

$$M_I = a_0 + a_1(I-J) + a_2(I-J)^2 + a_3(I-J)^3 + a_4(I-J)^4 \quad (1)$$

where a_0 = 11.370, a_1 = −19.175, a_2 = 21.587, a_3 = −7.877, a_4 = 0.9710, valid for $0.9 \leq I - J \leq 3.1$.

Reid & Cruz (2002) established a similar relation for the Cousins/CIT colours, which only differ slightly from the DENIS colours. That relation is illustrated in Fig. 1, together with the theoretical prediction of Baraffe (1998). In the [1.7, 3.1] range we could collect 22 data points, significantly more than the 14 objects that we count in Fig. 11 of Reid & Cruz (2002).

In the [1.0, 1.4] interval the three curves are very close, but they then disagree over the intermediate [1.4, 1.8] region where the colour-luminosity relation steepens considerably. Reid & Cruz (2002) choose to describe this difficult region by

Table 1. Single red dwarfs with accurate trigonometric parallaxes and good DENIS photometry, used for the absolute magnitude calibration.

Stars	α_{2000}	δ_{2000}	DENIS epoch	I	$I-J$	$J-K$	err$I$	err$J$	err$K$	π mas	errπ mas	M_I	Ref.
(1)	(2)	(3)	(4)	(5)	(6)	(7)	(8)	(9)	(10)	(11)	(12)	(13)	(14)
G 158-027	00 06 43.37	−07 32 10.5	1996.693	10.36	1.94	0.96	0.03	0.06	0.07	213.0	3.6	12.00	b
LHS 1026	00 09 04.32	−27 07 19.8	1999.833	9.77	1.08	0.65	0.03	0.06	0.07	42.8	2.6	7.93	a
HIP 1399	00 17 30.41	−59 57 04.3	1998.600	9.66	1.12	0.97	0.02	0.10	0.09	22.5	2.3	6.42	a
GJ 2003	00 20 08.37	−17 03 40.7	2000.589	9.70	1.21	0.77	0.03	0.08	0.10	39.3	3.1	7.67	a
GJ 1009	00 21 56.03	−31 24 21.9	1999.756	9.03	1.21	1.11	0.03	0.06	0.08	54.9	2.2	7.73	a
LHS 1064	00 23 18.55	−50 53 38.1	2000.860	9.52	1.19	0.89	0.04	0.08	0.09	47.4	2.8	7.90	a
BRI 0021-02*	00 24 24.63	−01 58 20.0	1998.734	15.13	3.26	1.31	0.04	0.10	0.09	82.5	3.4	14.71	b
LHS 1106	00 35 59.98	−09 30 56.0	2000.762	9.59	1.04	0.83	0.03	0.08	0.08	28.5	2.3	6.86	a
LHS 1122	00 39 58.88	−44 15 11.8	2000.688	9.48	1.19	0.83	0.03	0.09	0.07	43.6	2.6	7.68	a
LP 646-17	00 48 13.33	−05 08 07.4	2000.548	9.91	1.10	0.87	0.03	0.08	0.08	38.9	4.7	7.86	a
RGO 0050-2722	00 52 54.67	−27 05 59.5	1998.729	16.67	3.19	1.06	0.08	0.12	0.14	41.0	4.0	14.73	b
G 70-22	00 56 30.25	−04 25 15.0	2000.603	12.18	1.71	0.83	0.03	0.08	0.06	33.3	3.8	9.79	b
LP 706-69	00 56 50.41	−11 35 19.7	2000.603	9.63	1.35	0.89	0.03	0.08	0.06	41.7	2.5	7.73	a
G 268-110	01 04 53.70	−18 07 29.2	1998.718	11.09	1.72	0.97	0.03	0.10	0.09	99.8	5.0	11.09	b
LP 293-94	01 17 59.36	−48 09 01.0	1999.805	9.74	1.07	0.84	0.03	0.07	0.07	24.6	4.4	6.69	a
LP 707-58	01 18 15.97	−12 53 59.6	2000.575	9.60	1.19	0.96	0.03	0.06	0.07	45.2	3.6	7.88	a
L 367-82	01 41 03.64	−43 38 09.9	1998.923	9.90	1.03	0.87	0.04	0.06	0.08	23.7	2.6	6.77	a
LHS 6033	01 46 36.78	−08 38 57.4	1998.710	10.28	1.42	0.85	0.03	0.09	0.12	70.1	14.2	9.51	b
G 271-177	01 53 45.45	−06 03 02.1	1996.688	10.02	0.95	0.84	0.03	0.08	0.07	19.0	3.6	6.41	a
L 297-54	02 36 38.98	−46 54 18.8	1998.929	9.53	0.93	0.91	0.02	0.07	0.07	25.8	3.4	6.59	a
LHS 1426	02 37 29.71	+00 21 27.8	2000.838	12.10	1.51	0.90	0.03	0.07	0.08	40.2	4.3	10.12	b
LHS 1438	02 43 53.24	−08 49 46.0	2000.899	9.83	1.07	0.84	0.03	0.08	0.07	42.2	3.4	7.96	a
LHS 17	02 46 14.97	−04 59 21.5	2000.655	12.66	1.76	0.83	0.03	0.07	0.08	60.3	8.2	11.56	b
LP 771-21	02 48 40.98	−16 51 21.9	2000.803	15.29	2.73	1.20	0.04	0.08	0.10	59.5	5.4	14.16	c
T* 831-161058	02 51 13.25	+00 47 36.8	2000.901	16.51	2.74	1.19	0.08	0.11	0.14	20.5	2.2	13.07	b
T* 831-165166	02 51 42.68	−01 02 05.6	2000.896	16.52	2.29	1.09	0.08	0.12	0.18	19.5	3.9	12.97	c
LP 994-59	03 09 27.87	−42 28 50.7	1999.885	10.24	1.17	0.81	0.03	0.07	0.08	34.0	2.4	7.90	a
G 077-055	03 29 04.06	+01 40 07.8	2000.759	9.99	1.05	0.80	0.03	0.08	0.09	21.2	3.6	6.62	a
Gl 145	03 32 55.83	−44 42 07.1	1999.896	9.09	1.29	0.90	0.03	0.06	0.08	92.0	1.8	8.91	a
LHS 1565	03 35 59.61	−44 30 45.5	1998.753	9.53	2.00	0.77	0.03	0.10	0.14	273.4	5.2	11.71	e
LP 944-20	03 39 35.26	−35 25 43.6	2001.049	13.96	3.27	1.19	0.05	0.09	0.10	200.0	4.2	15.47	c
LHS 1604	03 51 00.03	−00 52 44.6	1999.907	13.75	2.56	0.99	0.03	0.07	0.09	68.1	1.8	12.92	b
LHS 1832	06 10 59.85	−65 12 20.3	1998.877	9.40	1.12	0.83	0.02	0.05	0.06	33.6	4.4	7.03	a
L 309-4	06 29 01.40	−45 21 59.2	2000.145	9.12	0.98	0.80	0.03	0.08	0.07	30.2	1.5	6.52	a
LP 839-11	06 32 08.83	−27 01 58.7	2001.085	9.70	1.06	0.88	0.03	0.07	0.07	37.0	2.6	7.54	a
LHS 1855	06 33 50.14	−58 31 45.6	1996.066	9.46	1.58	0.82	0.02	0.07	0.08	61.3	1.8	8.40	a
G 108-024	06 44 13.94	−00 55 31.5	1999.019	9.76	1.00	0.82	0.04	0.05	0.06	23.8	3.1	6.64	a
LHS 234	07 40 19.31	−17 24 45.5	1999.192	12.36	2.20	0.85	0.02	0.05	0.07	112.4	2.7	12.61	b
HIP 39436	08 03 40.87	−24 28 35.1	1998.964	9.63	0.94	0.74	0.03	0.05	0.11	22.2	3.1	6.36	a
L 98-45	08 19 16.07	−67 48 14.3	1996.964	10.16	1.01	0.86	0.02	0.05	0.06	26.9	2.4	7.31	a
LP 665-21	08 31 21.75	−06 02 01.4	1996.038	9.26	1.21	0.89	0.03	0.05	0.06	46.0	6.4	7.57	a
LHS 6149	08 34 25.91	−01 08 39.3	2000.022	10.11	1.34	0.69	0.02	0.06	0.06	73.4	9.6	9.44	b
LP 98-62	08 41 32.69	−68 25 40.6	1999.238	9.24	0.99	0.88	0.02	0.04	0.06	32.1	1.6	6.77	a
LHS 2145	09 28 53.34	−07 22 16.1	2000.326	9.69	1.28	0.76	0.03	0.07	0.07	58.2	4.1	8.51	a
LHS 2264	10 26 07.80	−17 58 43.5	1996.044	9.60	1.02	0.75	0.02	0.06	0.07	29.1	2.3	6.92	a
LHS 292	10 48 12.64	−11 20 09.8	2000.200	11.25	2.30	0.98	0.03	0.07	0.06	220.3	3.6	12.97	b
DENIS 1048-39	10 48 14.42	−39 56 08.2	2001.359	12.64	3.00	1.13	0.03	0.07	0.07	192.0	37.0	14.06	d
LP 672-4	11 09 12.28	−04 36 24.9	1999.378	9.49	1.40	0.77	0.03	0.06	0.06	39.9	2.4	7.49	a
LHS 2397a	11 21 49.21	−13 13 08.3	2000.501	14.97	3.09	1.25	0.10	0.11	0.08	70.0	2.1	14.09	b
LP 793-34^{+}	11 45 35.40	−20 21 05.2	2000.241	13.84	2.15	0.88	0.05	0.05	0.10	49.6	3.6	12.32	a
LHS 314	11 46 42.93	−14 00 51.8	2000.205	9.33	1.30	0.96	0.03	0.07	0.07	49.0	2.9	7.78	a
LHS 2475	11 55 07.44	+00 58 25.9	1996.208	9.39	1.18	0.87	0.03	0.05	0.07	35.8	3.2	7.16	a

discontinuities at $I-J=1.45$ and $I-J=1.65$, with a constant value with large error bars ($M_I=10.2\pm0.7$) used in-between. The discontinuities clearly are non-physical, but our polynomial fit, just as clearly, runs the risk of smoothing out a steeper intrinsic slope which could reflect a real physical change or transition in the stellar structure.

Table 1. continued.

Stars	α_{2000}	δ_{2000}	DENIS epoch	I	$I-J$	$J-K$	err$I$	err$J$	err$K$	π mas	errπ mas	M_I	Ref.
LHS 2477	11 55 49.22	−38 16 49.7	2001.104	9.88	1.12	0.75	0.03	0.07	0.09	42.8	3.0	8.04	a
LHS 2509	12 04 36.61	−38 16 25.2	2000.233	9.74	1.15	0.87	0.04	0.08	0.05	37.3	4.9	7.60	a
LP 794-30	12 11 11.78	−19 57 38.1	1999.148	9.48	1.57	0.89	0.03	0.05	0.08	78.1	3.1	8.94	a
LP 852-57	12 13 32.93	−25 55 24.5	1999.153	9.48	1.08	0.84	0.03	0.06	0.08	42.1	2.5	7.60	a
LHS 2587	12 36 49.29	−76 57 17.8	1998.197	9.37	0.96	0.85	0.02	0.07	0.07	27.8	1.7	6.59	a
LHS 2595	12 38 47.34	−04 19 17.0	1999.414	10.80	1.46	0.86	0.02	0.06	0.08	50.7	3.1	9.33	b
LP 617-37	13 20 24.96	−01 39 26.3	1999.211	9.57	1.23	0.85	0.03	0.06	0.09	48.2	2.9	7.98	a
LP 855-14	13 27 53.95	−26 57 01.8	2001.151	9.60	1.25	0.88	0.03	0.08	0.09	48.0	2.9	8.01	a
LHS 2770	13 38 24.73	−02 51 51.9	1999.279	12.54	1.43	0.95	0.04	0.07	0.07	26.3	6.7	9.64	b
LP 912-26	13 53 19.76	−30 46 37.6	2000.364	10.02	1.06	0.97	0.03	0.06	0.09	27.0	3.8	7.18	a
LHS 2876	14 12 12.17	−00 35 16.2	1999.444	15.59	2.50	1.01	0.05	0.08	0.08	32.7	4.1	13.16	c
T* 868-110639	15 10 16.86	−02 41 07.4	1999.384	15.73	3.09	1.32	0.05	0.07	0.09	57.5	1.9	14.53	b
LHS 392	15 11 50.60	−10 14 17.8	2000.277	11.24	1.47	0.90	0.04	0.09	0.12	67.4	3.1	10.38	b
LP 915-16	15 17 21.16	−27 59 49.8	1996.422	9.58	1.27	0.91	0.02	0.08	0.12	41.2	3.7	7.66	a
LHS 3092	15 36 34.53	−37 54 22.3	1999.211	9.91	1.47	0.79	0.03	0.05	0.06	81.6	13.7	9.47	b
LHS 3093	15 36 58.69	−14 08 00.7	1998.373	10.02	1.63	0.88	0.02	0.05	0.05	74.9	3.8	9.39	b
LP 336-71	15 49 38.34	−47 36 33.8	1999.290	9.46	1.13	0.88	0.03	0.05	0.06	37.5	2.6	7.33	a
LP 744-46	16 02 35.07	−14 38 36.5	1996.359	9.71	1.16	0.85	0.03	0.06	0.09	31.4	4.1	7.19	a
LHS 412	16 08 15.03	−10 26 11.7	1998.323	11.78	1.51	0.81	0.03	0.07	0.09	47.1	2.7	10.15	b
LHS 3185	16 22 40.97	−48 39 19.7	1999.570	9.70	1.26	0.78	0.04	0.08	0.05	41.0	3.7	7.76	a
LP 625-34	16 40 05.98	+00 42 19.3	1999.625	10.67	1.57	0.84	0.02	0.06	0.06	89.0	2.3	10.42	b
LHS 3242	16 48 24.40	−72 58 33.9	2000.537	9.27	1.22	0.80	0.03	0.08	0.06	62.7	1.9	8.25	a
LHS 3272	17 13 40.46	−08 25 14.6	2000.573	9.54	1.39	0.83	0.04	0.07	0.27	52.8	4.2	8.15	a
HIP 86938	17 45 53.36	−13 18 22.1	2000.551	10.14	1.06	0.81	0.04	0.08	0.06	26.9	3.8	7.29	a
HIP 91644	18 41 19.73	−60 25 47.4	2000.381	9.45	1.01	0.76	0.02	0.06	0.09	27.5	2.5	6.65	a
LHS 3421	18 52 52.30	−57 07 38.1	2000.773	9.84	1.35	0.89	0.03	0.07	0.07	37.5	3.8	7.71	a
L 850-62	19 03 16.64	−13 34 05.4	2000.573	11.93	1.57	0.81	0.03	0.07	0.07	52.4	3.8	10.53	b
LTT 7598	19 12 25.27	−55 52 07.6	1999.512	9.47	1.19	0.87	0.02	0.05	0.06	50.0	2.5	7.97	a
LP 635-46	20 43 41.32	−00 10 41.3	1999.605	9.54	1.02	0.88	0.02	0.06	0.07	38.4	3.1	7.46	a
LP 211-96	20 59 51.36	−58 45 31.1	2001.359	9.71	1.14	0.85	0.04	0.08	0.07	32.0	2.9	7.24	a
LHS 3639	21 11 49.56	−43 36 48.8	1999.540	9.59	1.14	0.77	0.08	0.08	0.07	69.8	4.2	8.81	a
LHS 3666	21 24 18.32	−46 41 35.3	1999.559	10.20	1.20	0.86	0.03	0.06	0.07	37.2	4.8	8.05	a
HB 2124-4228	21 27 26.12	−42 15 18.1	1998.652	16.02	2.47	1.45	0.06	0.13	0.16	28.0	6.2	13.26	c
HIP 106043	21 28 44.42	−47 15 42.2	1998.501	10.36	1.04	0.98	0.05	0.11	0.12	26.7	4.0	7.49	a
LHS 513	21 39 00.66	−24 09 26.7	1996.638	10.68	1.55	0.74	0.04	0.06	0.08	73.3	12.0	10.01	b
LHS 5374	21 54 45.25	−46 59 34.5	2000.605	9.73	1.32	0.88	0.03	0.08	0.08	66.1	3.3	8.83	a
HIP 108523	21 59 08.30	−46 45 47.3	1998.679	9.74	1.10	1.03	0.03	0.11	0.11	37.8	3.8	7.63	a
LP 283-3	22 03 27.19	−50 38 39.2	2000.512	9.83	1.14	0.87	0.04	0.07	0.14	45.9	8.3	8.14	a
LHS 3776	22 13 42.90	−17 41 08.8	2000.504	10.65	1.70	0.84	0.08	0.06	0.06	96.0	3.9	10.56	b
T* 890-60235	22 23 05.56	+00 30 11.1	1999.614	16.62	2.43	1.18	0.07	0.10	0.14	19.4	2.2	13.06	c
HIP 110655	22 25 02.83	−33 12 16.2	2000.458	9.02	0.92	0.75	0.04	0.08	0.08	30.7	5.2	6.46	a
LHS 523	22 28 54.38	−13 25 17.8	1998.729	12.87	2.19	0.89	0.04	0.11	0.13	88.8	4.9	12.61	b
LHS 526	22 34 53.61	−01 04 58.0	1998.723	11.89	1.47	1.04	0.03	0.09	0.17	42.5	3.7	10.03	b
LHS 3850	22 46 26.28	−06 39 25.0	1998.474	12.62	1.94	0.80	0.02	0.10	0.12	53.3	4.6	11.25	b
HIP 114252	23 08 19.55	−15 24 35.8	1999.466	9.17	1.15	0.93	0.02	0.07	0.06	45.8	2.7	7.47	a
G 157-52	23 21 11.25	−01 35 44.9	2000.578	9.77	1.11	0.82	0.03	0.07	0.08	37.0	3.7	7.61	a
LHS 546	23 35 10.45	−02 23 19.9	1999.696	11.01	1.87	0.97	0.03	0.07	0.07	138.3	3.5	11.71	b
HIP 118180	23 58 22.03	−53 48 33.6	1999.874	9.21	0.97	0.68	0.03	0.07	0.07	29.7	3.0	6.57	a

T* TVLM.

$^+$ Hipparcos, for LP 793-33.

* BRI 0021-02. This object is also listed in the NLTT, as LP 585-86. That name is clearly an NLTT typo: another star (the much brighter HIP 3061) bears the same name, with coordinates that are consistent with the LP numbering sequence. The NLTT proper motion is on the other hand valid: 0.212, 320 degrees.

Columns 1–4: object name, DENIS Position for equinox J2000 at DENIS epoch, and DENIS epoch.

Columns 5–7; and 8–10: DENIS *I*-magnitude and colours; and associated standard errors.

Columns 11, 12: trigonometric parallax and its standard error.

Column 13: M_I absolute magnitude, calculated from DENIS *I*-magnitude and parallax.

Column 14: parallax reference: (a) HIP; (b) GCTP; (c) Tinney et al. (1995) and Tinney (1996); (d) Deacon & Hambly (2001); (e) Henry et al. (1997).

Which of the two description is preferable largely rests on a small group of stars in this colour range: LHS 1855 (Gl 238), LP 794-30, LHS 3093 (Gl 592), G 70-22, and to a lesser extend, LHS 3850 (GJ 4294). If those stars are single, the polynomial fit is clearly preferable to the Reid & Cruz prescription, but an alternative hypothesis is that they are photometric binaries. Of the five, two have been examined for companions (LHS 1855, Scholz et al. 2000; LHS 3093, Skrutskie et al. 1989) and found single, but only with seeing-limited resolution. LP 794-30 has a known companion, but at 85″, outside any photometric diaphragm. We observed both G 70-22 and LHS 3850 with adaptive optics at CFHT, and found the former resolved with $\Delta(K) = 1.5$ at a separation of 0.8″. For now we lack objective reasons to excise the other 4 stars from the list and have thus left them in, but we did add them to the observing lists of our adaptive optics and radial velocity programs (Delfosse et al. 1999).

In the $I - J$ range of primary interest here ([2.0,3.0]) all three relations again agree well with the data, as seen in Fig. 2 which plots the residuals of the observed data points from the three fits. Over the $[1.9, 3.1]$ range the rms dispersion of the data around our fit is 0.26, corresponding to a 12% error on distances; it is respectively 0.30 and 0.31 for the Baraffe et al. (1998) and Reid & Cruz (2002) relations. Over the $[2.0, 3.0]$ range the Eq. (1) polynomial is therefore a small but significant improvement, and we use it for the reminder of this paper.

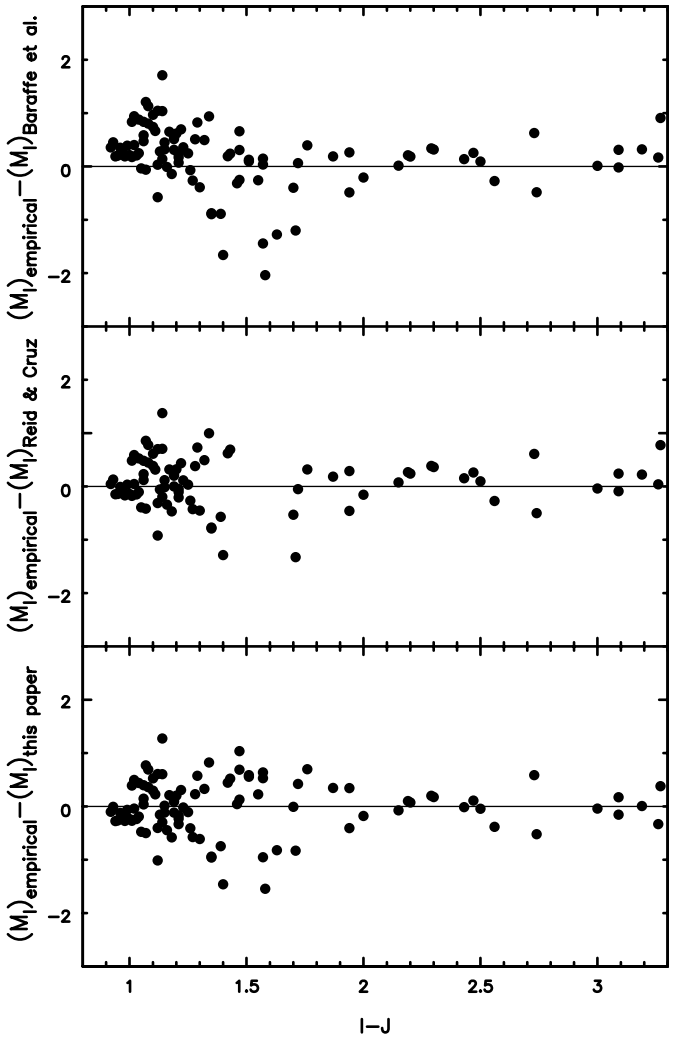

Fig. 2. Empirical M_I absolute magnitudes compared with values obtained from the theoretical tracks of Baraffe et al. (1998; top), from the piecewise polynomial calibration of Reid & Cruz (2002; middle) (except for $1.45 < I - J < 1.65$), and from the calibration derived in this paper (bottom).

3. Sample selection

3.1. Star selection from the DENIS survey

We systematically search the DENIS database (available at the Paris Data Analysis Center, PDAC) for potential members of the solar neighbourhood, with simple and well defined criteria. Specifically, we start by selecting all high galactic latitude DENIS sources ($|b_{II}| \geq 30°$) that are redder than $I - J = 1.0$ (approximately the colour of an M0 dwarf, Leggett 1992). We then compute photometric distances to retain stars with $D_{\rm phot} < 30$ pc. We used the Paper I colour-magnitude relation for this selection since the colour-relation presented above was not yet available when we queried the DENIS database, but later recomputed all distances with the new relation.

When the search program was last run in mid-2001, 5700 square degrees (slightly over half of the southern high galactic latitude sky) were available in the database (Delfosse & Forveille 2001). 2100 of those 5700 square degrees had been considered in Paper I and are reanalysed here with slightly improved tools, and 3600 square degrees are new. The number of potential early-M dwarfs (M 0 to M 6, $1.0 \leq I - J \leq 2.0$) with photometric distances within 30 pc is significantly larger (~5000) than the total population expected for the sampled volume (~1400, Henry et al. 2002), and therefore must be dominated by contamination from distant M-giants with similar colours. Its analysis will require considerable follow-up, which is beyond the scope of the present work. Very late-M and L dwarfs ($I - J \geq 3.0$) will be considered in a forthcoming paper (Delfosse et al., in preparation). As in Paper I, we thus restrict the present analysis to stars in the $2.0 \leq I - J \leq 3.0$ colour interval, or approximately to spectral types M 6 to M 8.

At that stage in the selection, the candidate sample contains approximately equal numbers of nearby dwarfs and distant giants. A cut in the $I - J/J - K$ colour-colour diagram (Fig. 3) rejects a sizeable fraction of the giants, but the DENIS photometry is not sufficiently accurate to eliminate all of them without losing some dwarfs. That step needs proper motion information, and is discussed in Sect. 5.

3.2. Searching in the NLTT catalogue

To extend our search to lower galactic latitudes, we turned to known high proper motion stars, and looked for faint NLTT (Luyten 1980) stars with DENIS colours and magnitudes compatible with a nearby late M-dwarf. As the brighter NLTT stars have usually been better characterised, we restricted that search to NLTT stars fainter than $R_{\rm Luyten} = 14.0$ and redder than

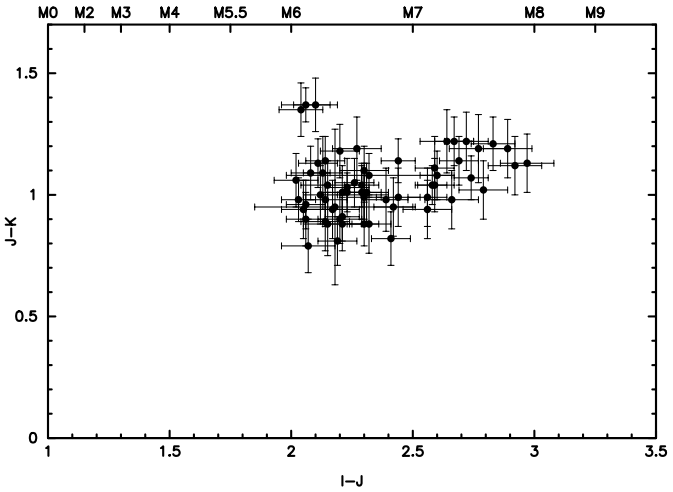

Fig. 3. DENIS colour-colour diagram for all 62 late-M dwarf candidates detected in the 5700 square degrees (Paper I and this paper) so far examined in DENIS. Stars selected from the NLTT outside this area are not shown. The (indicative) spectral type labels on the top axis are adopted from Leggett (1992).

$(B–R)_{\rm Luyten} = 1.5$ (approximately later than M1, Leggett 1992). The resulting 7424 stars were searched for in the 14 000 square degrees of DENIS data that are presently processed and available on-line at PDAC. This cross-identification is made somewhat difficult by the interplay of crowded fields at low galactic latitudes with the often poor coordinates of the southern stars in the NLTT catalogue. We therefore expect to have missed some significant fraction of the true matches. These NLTT stars were then handled as those extracted directly from DENIS, except that they obviously were ignored during the statistical analysis of the DENIS sample. We present here 15 candidates matching our previous criteria ($2.0 \leq I - J \leq 3.0$; and photometric distance within 30 pc).

4. Proper motions and *B*, *R* magnitudes

We searched for plates containing the dwarf candidates in the collection of the Centre d'Analyse des Images (CAI, `http://www.cai-mama.obspm.fr/`): POSS I ($-30° < \delta < 0°$), SRC-J ($-90° < \delta < 0°$), SRC-R ($-17° < \delta < 0°$) and ESO-R ($\delta < -17°$), depending on the declination. We then used the MAMA microdensitometer (Berger et al. 1991) at CAI to digitize the survey plates, and analysed the resulting images with SExtractor (Bertin & Arnouts 1996). We calibrated these measurements using the ACT (Urban et al. 1998) and GSPC-2 (Postman et al. 1997; Bucciarelli et al. 2001) catalogues, as respectively astrometric and photometric references.

A least-square fit to the positions at the 3 to 4 available epochs (including the DENIS survey epoch), determines absolute proper motion. The time baseline spans 13 to 49 years, and results in proper motion standard errors of 29 to 7 mas/year. The photometric standard errors are ±0.3 mag for *B* and ±0.2 mag for *R*. Tables 2a and 2c respectively list the proper motion determinations for 24 high proper motions (high-PM, $\mu > 0.1''$ yr^{-1}) in the 3600 square degrees and 11 lower proper motions (low-PM, $\mu < 0.1''$ yr^{-1}) in the full 5700 square degrees. Table 2b lists the proper motions for 15 high-PM candidates initially selected from the NLTT catalog.

Table 2. a) Proper motions of the 24 high-PM ($\mu > 0.1''$ yr^{-1}) late-M dwarfs selected in the 3600 square degrees.

DENIS name	μ_α [$''$ yr^{-1}]	μ_δ [$''$ yr^{-1}]	$\mu_{\rm total}$ [$''$ yr^{-1}]	$\mu_{\rm L}$ [$''$ yr^{-1}]
J0020231−234605	+0.322	−0.066	0.329	0.370
J0103119−535143*	−0.094	−0.218	0.238	...
J0120491−074103*	−0.013	−0.115	0.116	...
J0144318−460432*	+0.117	−0.049	0.127	...
J0218579−061749	+0.367	−0.097	0.379	0.375
J0235495−071121*	+0.284	+0.093	0.299	...
J0306115−364753*	−0.181	−0.700	0.723	...
J0320588−552015*	+0.302	+0.259	0.398	...
J0351000−005244	+0.035	−0.475	0.477	0.525
J0517377−334903*	+0.464	−0.342	0.576	...
J1006319−165326	−0.318	+0.181	0.366	0.391
J1021513−032309	+0.202	−0.147	0.249	0.269
J1048126−112009	+0.604	−1.521	1.637	1.644
J1106569−124402	−0.314	+0.001	0.314	0.355
J1141440−223215*	−0.141	+0.400	0.424	...
J1145354−202105	+0.149	+0.063	0.161	0.186
J1147421+001506	−0.262	−0.083	0.275	0.303
J1155429−222458	−0.377	−0.185	0.420	0.412
J1201421−273746	−0.289	−0.187	0.344	0.302
J1250526−212113*	+0.441	−0.340	0.557	...
J1610584−063132	−0.051	−0.180	0.187	0.229
J2132297−051158	+0.109	−0.337	0.354	0.350
J2205357−110428	−0.271	−0.166	0.318	0.339
J2337383−125027	+0.205	−0.312	0.373	0.365

* Not previously known as a high-PM star.
Column 1: object name.
Columns 2–4: μ_α, μ_δ, $\mu_{\rm total}$, our measurements, in arcsec yr^{-1}.
Column 5: total proper motion from Luyten (1979, 1980), when available.

For some bright low-PM objects, we used *B* and *R* magnitudes available in the USNO-A2.0 catalogue (Monet et al. 1998), as well as more accurate proper motions from the UCAC1 (Zacharias et al. 2000) & Tycho-2 (Høg et al. 2000) catalogues.

5. Reduced proper motions

In Paper I probable giants were rejected on a proper motion cutoff, by requiring $\mu \geq 0.1''$ yr^{-1}. This criterion, while effective, is not optimal, in that it completely ignores the photometric information: an apparently fainter star, everything else being equal, is farther away than a brighter one, and is thus on average expected to have a smaller proper motion. The combination of kinematic and photometric information embodying that simple idea is the Reduced Proper Motion (RPM), extensively used by Luyten and initially coined by Hertzsprung. The RPM is defined in terms of the observable parameters as:

$$H = m + 5 + 5\log\mu \qquad (2)$$

Table 2. b) Proper motions of the 15 high-PM ($\mu > 0.1''$ yr^{-1}) late-M dwarfs initially selected from the NLTT (same Cols. as Table 2a).

DENIS name	μ_α [$''$ yr^{-1}]	μ_δ [$''$ yr^{-1}]	$\mu_{\rm total}$ [$''$ yr^{-1}]	$\mu_{\rm L}$ [$''$ yr^{-1}]
J0002061+011536	+0.474	+0.068	0.479	0.445
J0410480−125142	−0.117	−0.382	0.400	0.426
J0440231−053009	+0.313	+0.101	0.329	0.243
J0520293−231848	+0.222	+0.250	0.334	0.334
J0931223−171742	−0.286	−0.131	0.315	0.296
J1346460−314925	−0.336	+0.158	0.372	0.371
J1504161−235556	−0.317	−0.078	0.326	0.322
J1546115−251405	−0.218	−0.310	0.379	0.377
J1552446−262313	+0.227	−0.475	0.526	0.492
J1553571−231152	−0.112	−0.281	0.303	0.299
J1625503−240008	−0.158	−0.026	0.161	0.184
J1641430−235948	−0.111	−0.185	0.216	0.212
J1645282−011228	+0.013	−0.220	0.220	0.231
J1917045−301920	+0.191	−0.207	0.281	0.212
J2151270−012713	+0.220	+0.023	0.221	0.223

where m is the apparent magnitude in a given photometric band and μ is the total proper motion in arcsec yr^{-1}. Its usefulness becomes more apparent after it is rephrased in terms of intrinsic stellar parameters, to:

$$H = M + 5\log(V_{\rm t}/4.74) \quad (3)$$

where M is the absolute magnitude in the same photometric band and $V_{\rm t}$ is the tangential velocity (km s^{-1}). Under this form it is clear that, unless it serendipitously has a very unusually low tangential velocity, a dwarf will have a much larger RPM than any giant. Subdwarfs have even larger RPMs than normal dwarfs, through a combination of fainter magnitudes (at a given colour) and a larger velocity dispersion. RPM vs. colour plots are therefore extremely effective at statistically separating giants, dwarfs, subdwarfs, and white dwarfs.

The largest possible $V_{\rm t}$ for a star bound to the Galaxy is that of a retrograde star orbiting at the escape velocity, and located in the direction of either the galactic center or anticenter:

$$V_{\rm max} = V_{\rm e} + V_{\rm LSR} + V_\odot \quad (4)$$

where:

- $V_{\rm e}$ ~500 ± 40 km s^{-1} is the escape velocity in the solar neighbourhood (Leonard & Tremaine 1990; Meillon 1999),
- $V_{\rm LSR}$ ~220 km s^{-1} (Kerr & Lynden-Bell 1986) is the rotation velocity of the Local Standard of Rest,
- $V_\odot$ ~5 km s^{-1} (Dehnen & Binney 1998) is the solar velocity relative to the LSR.

Taking safe margins on all components, $V_{\rm max}$ is thus at most 800 km s^{-1}. For a given stellar luminosity, and in the I photometric band, this translates into a maximum RPM of:

$$H_I^{\rm max} = M_V - (V-I) + 5\log(V_{\rm max}/4.74). \quad (5)$$

To estimate the maximum RPM for giants at a given colour, we fitted polynomial functions to the $V-I$ and $I-J$ colours data from Thé et al. (1990), Bessell & Brett (1988), and used Eq. (5) to obtain:

$$H_I^{\rm max} = 18.82 - 9.97(V-I) + 2.83(V-I)^2 - 0.25(V-I)^3 \quad (6)$$

for $V-I \in [1.5, 5.0]$

$$H_I^{\rm max} = 18.97 - 17.04(I-J) + 8.08(I-J)^2 - 1.22(I-J)^3 \quad (7)$$

for $I-J \in [1.0, 3.0]$.

Figure 4 shows the resulting $H_I^{\rm max}$ vs. $(V-I)$ and vs. $(I-J)$ curves, and our candidates.

To produce the (H_I, $V-I$) diagram, we interpolated a very approximate V-magnitude from the the B and R photographic magnitudes. This is obviously very crude, but nonetheless proves adequate: the $H_I^{\rm max}$ vs. $V-I$ curve for giants is fairly flat, so that even large errors on $V-I$ do not significantly affect

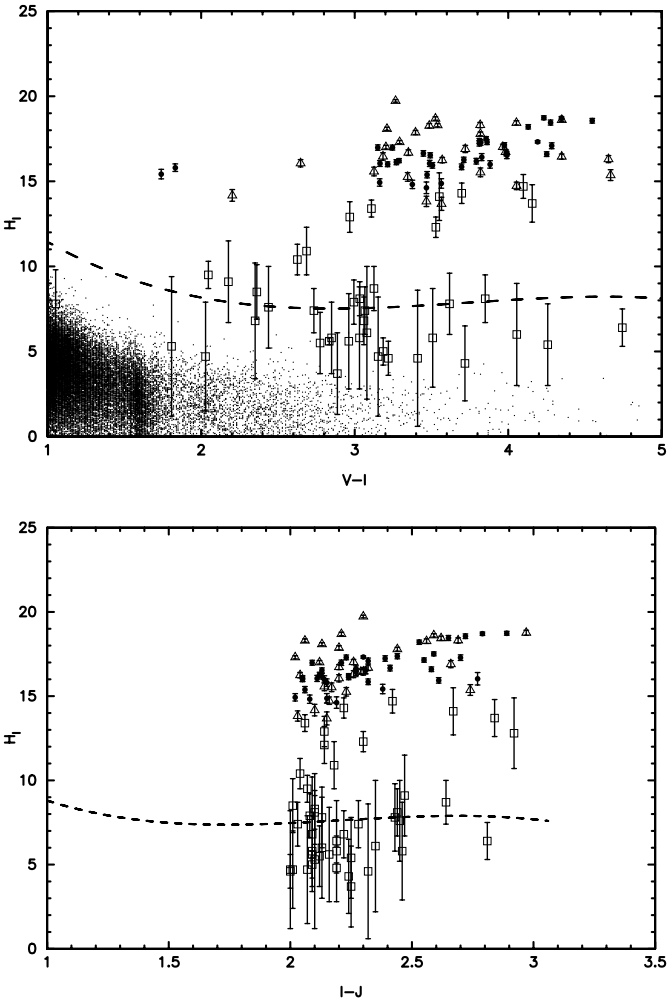

Fig. 4. I band reduced proper motions vs. $V-I$ and $I-J$. Dashed curve: $H_I^{\rm max}$ for giants. Objects above this curve must be dwarfs. Solid circles: high-PM objects in this paper, Tables 3a, 3b; Triangles: late-M dwarf candidates from Paper I (Table 2); Squares: low-PM objects, Tables 3c and 4. In the upper diagram, the many dots are HIPPARCOS single giants with $V-I \geq 1.0$ (28 022 stars), all of which are located well below the dwarf/giant separation curve.

Table 2. c) Proper motions of 11 low-PM ($\mu < 0.1''$ yr^{-1}) probable late-M dwarfs found in the 5700 square degrees.

DENIS name	μ_α [mas yr^{-1}]	μ_δ [mas yr^{-1}]	err μ_α [mas yr^{-1}]	err μ_δ [mas yr^{-1}]	$\mu_{\rm total}$ [mas yr^{-1}]
J0013093−002551	+97	+4	25	25	97
J0100021−615627	+78	−41	21	21	88
J0436278−411446	+22	+4	18	18	22
J0518113−310153	+41	−5	10	10	41
J1236396−172216	+14	−60	20	20	62
J1538317−103850	−8	−18	9	9	20
J1552237−033520	−8	−30	9	9	31
J1553186−025919	+14	−24	8	8	28
J2022480−564556	−1	−84	17	17	84
J2206227−204706	+28	−57	29	29	64
J2226443−750342	+48	+14	19	19	50

the position relative to the curve. As an illustration of the very effective giant/dwarf separation in RPM plots, the diagram also displays 28 000 single Hipparcos giants with adequate colour information, which all do lay well below the giants curve.

We divide the photometric candidates into 3 categories, plotted in Fig. 4, according to their position relative to the $H_I^{\rm max}$ curve:

- Stars with $\mu > 0.1''$ yr^{-1} are listed in Tables 2a and 3a (24 objects). As expected from the conservative limits used in Paper I, they are well above the giants curve, and have standard errors on H_I of ∼0.1. Figure 5 gives finding charts for the 9 completely new objects;
- Stars with $\mu < 0.1''$ yr^{-1}, but with $H_I - H_I^{\rm max} > 1\sigma$, with σ the uncertainty on H_I (11 objects, Table 3c). Their proper motions (Table 2c) have large relative uncertainties, and, because of the logarithmic μ dependency, their RPM measurements are thus quite noisy. A few of the noisiest and/or closest to the giants curve might possibly be giants, but the vast majority are dwarfs. One, DENIS-P J2206227−204706, detected in Paper I and ignored there because of its small proper motion, was in fact independently recognized as a late-M dwarf by Gizis et al. (2000);
- Stars with $H_I - H_I^{\rm max} < 1\sigma$ (Table 4), are overwhelmingly giants, with a minor admixture of very low tangential velocity dwarfs. The well known K5 dwarf Gl 710, for instance, lies outside our spatial and colour coverage, but with $H_I = 0.23$ it otherwise lays firmly within the "giants" region of the RPM diagram. This list (52 objects) includes a number of bright stars referenced as giants in the SIMBAD database. Our measured proper motions for those stars are usually not significant. This results in error bars on H_I that are occasionally so large (up to 5 mag) that some objects could not be included in Fig. 4 without obliterating the diagram. Whenever possible (i.e. for the brightest objects), we therefore replaced our own measurements by the much better proper motions available in the UCAC1 (Zacharias et al. 2000) and Tycho-2 (Høg et al. 2000) catalogues.

The 114 star sample identified by the photometric criteria ($2 \le I - J \le 3$, $d_{\rm phot} < 30$ pc) within the 5700 square degrees search area can therefore be divided into:

- 50 new nearby late-M dwarfs, consisting of:
  + 18 stars already found in high-PM catalogues (NLTT, WT, ...) but without previous distance estimate.
  + 32 completely new discoveries (13 in Paper I; 19 in this paper).
- 12 previously known nearby stars (2 in Paper I; 10 in this one).
- 52 probable giants, or dwarfs with very small PM.

The 50 new nearby late-M dwarfs represent a very significant addition to the known sample of 12 in this part of the sky. Our setting of the limiting distance to 30 pc rather than 25 pc (to avoid losing true $d < 25$ pc to distance errors) accounts for some but not most of this increase.

The 15 high-PM red dwarfs initially selected from NLTT are also listed in Tables 2b and 3b.

Tables 5a and 5b summarize the available physical parameters of the red dwarfs candidates listed in Tables 3a and 3b (DENIS origin) and 3c (NLTT origin): absolute magnitude M_I, distance, tangential velocity, and the approximate effective temperature derived from $I - J$ (Sect. 7). Two new late-M dwarfs have distance estimates within 10 pc in this paper: DENIS-PJ1552237−033520 and LP 860-41 (DENIS-P J1552446−262313). Five additional new stars are closer than 15 pc: DENIS-P J0306115−364753; LP 851-346 (DENIS-P J1155429−222458); DENIS-P J1250526−212113; LP 788-1 (DENIS-P J0931223−171742) and LP 911-56 (DENIS-P J1346460−314925).

Table 6 compares our distance determinations with litterature values for the 10 stars with a previous measurement or estimate. The agreement is generally good, except for a slight systematic discrepancy with Cruz & Reid 2002: for the 5 stars in common the Cruz & Reid distances are significantly larger. For the one star with three determinations, LP 655-48, our estimate and that of McCaughrean et al. (2002) agree and are both smaller than the Cruz & Reid distance.

6. Sample completeness, and the local late-M dwarf density

Since the stars which were initially fetched from proper motion catalogues have a very different (and poorly controlled) selection function, we restrict the discussion in this section to the colour-selected dwarf candidates in the full 5700 square degrees (this paper and Paper I). We also ignore the 52 probable giants of Table 4, which are of a different physical nature, and

Table 3. a) Observational data and Reduced Proper Motions for 24 high-PM nearby late-M dwarf candidates selected in the 3600 square degrees.

DENIS name	Other name	α_{2000}	δ_{2000}	DENIS epoch	B	R	I	$I-J$	$J-K$	H_I	$H_I^{\max}$
(1)	(2)	(3)	(4)	(5)	(6)	(7)	(8)	(9)	(10)	(11)	(12)
J0020231−234605	LP 825-35	00 20 23.17	−23 46 05.7	2000.589	20.4	17.5	14.65	2.39	0.98	17.2	7.8
J0103119−535143	...	01 03 11.98	−53 51 43.6	1999.879	20.1	17.5	14.54	2.27	1.19	16.4	7.7
J0120491−074103	...	01 20 49.15	−07 41 03.5	1999.926	**	19.4	15.71	2.77	1.19	16.0	7.9
J0144318−460432	...	01 44 31.88	−46 04 32.1	1999.882	19.3	16.7	14.10	2.19	0.81	14.6	7.6
J0218579−061749	LP 649-93	02 18 57.90	−06 17 49.7	2000.551	21.5	19.0	15.56	2.65	1.22	18.5	7.9
J0235495−071121	...	02 35 49.56	−07 11 21.1	1999.912	21.0	18.0	14.71	2.32	1.01	17.1	7.7
J0306115−364753	...	03 06 11.57	−36 47 53.2	1999.975	20.9	17.7	14.41	2.79	1.03	18.7	7.9
J0320588−552015	...	03 20 58.85	−55 20 15.8	1999.890	20.1	17.2	14.30	2.23	1.03	17.3	7.7
J0351000−005244	GJ 3252	03 51 00.03	−00 52 44.6	1999.907	19.8	16.7	13.75	2.55	0.99	17.1	7.9
J0517377−334903	...	05 17 37.70	−33 49 03.2	1999.962	21.1	18.2	14.93	2.89	1.19	18.7	7.8
J1006319−165326	LP 789-23	10 06 31.99	−16 53 26.3	2000.164	20.3	17.4	14.55	2.44	1.14	17.4	7.8
J1021513−032309	LP 610-5	10 21 51.36	−03 23 09.6	2000.260	20.0	17.8	14.55	2.31	0.88	16.5	7.7
J1048126−112009	GJ 3622	10 48 12.64	−11 20 09.8	2000.200	16.9	14.7	11.25	2.30	0.98	17.3	7.7
J1106569−124402	LP 731-47	11 06 56.91	−12 44 02.2	2000.247	19.9	17.3	14.18	2.41	0.82	16.7	7.8
J1141440−223215	...	11 41 44.06	−22 32 15.1	2000.258	21.7	19.1	15.42	2.72	1.21	18.6	7.9
J1145354−202105	LP 793-34*	11 45 35.40	−20 21 05.2	2000.241	19.0	16.6	13.84	2.15	0.88	14.9	7.6
J1147421+001506	GJ 3686B	11 47 42.11	+00 15 06.4	2000.197	18.6	15.7	13.19	2.06	0.96	15.4	7.5
J1155429−222458	LP 851-346	11 55 42.94	−22 24 58.2	1996.208	19.6	16.8	13.48	2.58	1.05	16.6	7.9
J1201421−273746	LP 908-5	12 01 42.10	−27 37 46.5	1999.129	19.8	16.3	14.30	2.21	0.91	17.0	7.6
J1250526−212113	...	12 50 52.66	−21 21 13.9	2000.249	19.3	16.8	13.78	2.59	1.11	17.5	7.9
J1610584−063132	LP 684-33	16 10 58.45	−06 31 32.2	2000.553	18.5	16.0	13.46	2.08	1.09	14.8	7.5
J2132297−051158	LP 698-2	21 32 29.76	−05 11 58.9	2000.408	19.1	16.3	13.52	2.12	1.13	16.3	7.6
J2205357−110428	LP 759-25	22 05 35.74	−11 04 28.5	1998.816	19.4	16.5	13.67	2.13	0.99	16.2	7.6
J2337383−125027	LP 763-3	23 37 38.33	−12 50 27.3	1998.805	19.1	16.2	13.67	2.13	1.10	16.5	7.6

* A companion to HIP 57361.

** Too faint for the Schmidt plates.

Columns 1, 2: object name in the DENIS data base, and other identification if available.

Columns 3–5: DENIS Position with respect to equinox J2000 at DENIS epoch, and DENIS epoch.

Columns 6, 7: B and *R* photographic magnitudes.

Columns 8–10: DENIS *I*-magnitude and colours.

Columns 11, 12: I band Reduced Proper Motion, and maximum RPM for an M giant of the same $I-J$ colour.

Table 3. b) Observational data and Reduced Proper Motions for 15 high-PM nearby late-M dwarf candidates initially selected from the NLTT (same Cols.as Table 3a).

DENIS name	Other name	α_{2000}	δ_{2000}	DENIS epoch	B	R	I	$I-J$	$J-K$	H_I	$H_I^{\max}$
(1)	(2)	(3)	(4)	(5)	(6)	(7)	(8)	(9)	(10)	(11)	(12)
J0002061+011536	LP 584-4	00 02 06.18	+01 15 36.6	1998.570	20.8	18.0	14.80	2.53	1.11	18.2	7.9
J0410480−125142	LP 714-37	04 10 48.06	−12 51 42.7	2000.896	17.8	15.4	12.99	2.05	1.05	16.0	7.5
J0440231−053009	LP 655-48	04 40 23.17	−05 30 09.1	1996.044	19.0	15.8	13.35	2.61	1.19	15.9	7.9
J0520293−231848	LP 836-41	05 20 29.37	−23 18 48.4	1999.847	19.2	16.6	14.02	2.27	1.12	16.6	7.7
J0931223−171742	LP 788-1	09 31 22.30	−17 17 42.4	2000.186	19.2	16.0	13.36	2.32	1.01	15.9	7.7
J1346460−314925	LP 911-56	13 46 46.07	−31 49 25.8	1999.301	18.0	15.8	13.27	2.24	1.07	16.1	7.7
J1504161−235556	LP 859-1	15 04 16.15	−23 55 56.4	2001.436	20.0	17.8	14.72	2.70	1.10	17.3	7.9
J1546115−251405	LP 860-30	15 46 11.53	−25 14 05.9	2001.400	19.0	16.5	14.09	2.09	0.89	17.0	7.5
J1552446−262313	LP 860-41	15 52 44.61	−26 23 13.7	1999.534	17.7	15.0	12.61	2.24	1.07	16.2	7.7
J1553571−231152	LP 860-46	15 53 57.14	−23 11 52.2	1996.301	18.4	16.0	13.64	2.05	1.02	16.0	7.5
J1625503−240008	LP 862-26	16 25 50.33	−24 00 08.5	1999.463	18.0	15.2	14.39	2.38	1.39	15.4	7.8
J1641430−235948	LP 862-111	16 41 43.00	−23 59 48.5	2000.545	17.9	15.0	14.13	2.15	1.20	15.8	7.6
J1645282−011228	LP 626-2	16 45 28.20	−01 12 28.8	2000.474	20.1	17.2	14.28	2.14	0.94	16.0	7.6
J1917045−301920	LP 924-17	19 17 04.51	−30 19 20.1	1999.353	19.1	16.4	13.81	2.11	0.95	16.1	7.6
J2151270−012713	LP 638-50	21 51 27.02	−01 27 13.7	2000.718	17.9	15.6	13.21	2.02	0.81	14.9	7.5

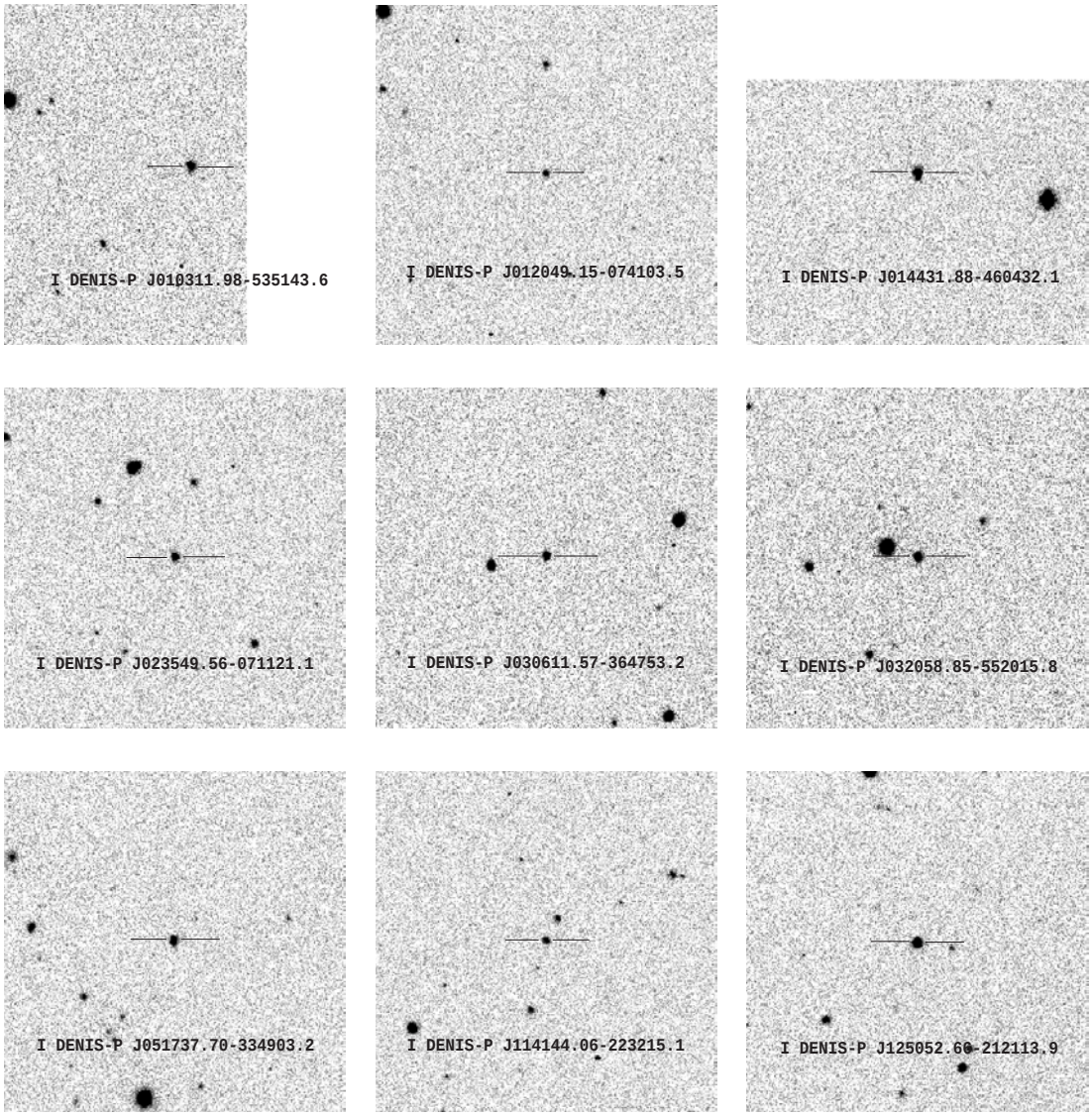

Fig. 5. *I*-band finding charts for the 9 new high-PM objects listed in Table 2a. The charts are ∼4.0′ × 4.0′, with North up and East to the left. No finding charts are provided for the lower proper motion objects, which are easily identified from their accurate coordinates.

therefore use a sample of 62 late-M dwarfs in the density calculation:

- 26 colour-selected high-PM stars from the 2100 square degrees explored in Paper I (Table 2, excluding 4 stars fetched from the LHS outside this area);
- 25 colour-selected high-PM stars from the additional 3600 square degrees explored here (Table 3a). This includes the colour-selection of LHS 5165, identified in Paper I from the LHS catalog and which happens to lay within the additional sky coverage;
- 11 colour-selected lower proper motion probable dwarfs, found over the full 5700 square degrees (Table 3c).

The differential photometric distance distribution of that sample (Fig. 6) is well fitted by a d^2 distribution, as expected for a constant-density population, out to ∼22–25 pc. The difference from the initial 30 pc selection cutoff reflects the slightly different colour-magnitude relations used in the selection and in the final photometric distance estimate. We conservatively

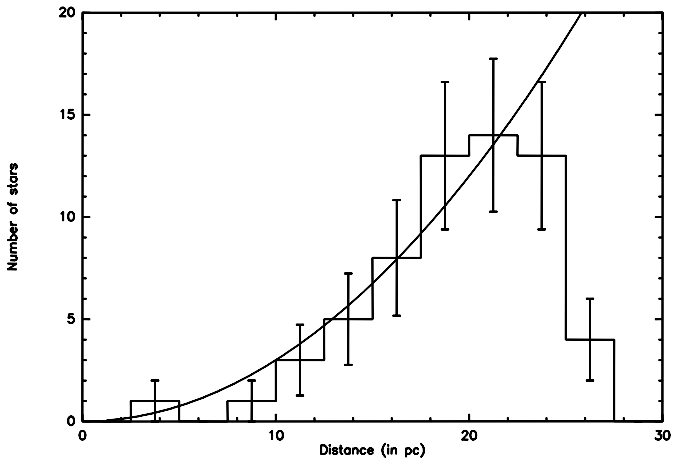

Fig. 6. Number of red dwarf candidates per 2.5 pc photometric distance bin over 5700 square degrees. The errorbars are Poissonian 1σ errors and the curve is the expected d^2 distribution, normalized at 18 pc.

Table 3. c) Observational information and Reduced Proper Motions for the 11 low-PM ($\mu < 0.1''$ yr^{-1}) red dwarfs candidates with $H_I - H_I^{\max} > 1\sigma$ in the full 5700 square degrees.

DENIS name	α_{2000}	δ_{2000}	DENIS epoch	B	R	I	$I-J$	$J-K$	H_I	err H_I	$H_I^{\max}$	Ref.
(1)	(2)	(3)	(4)	(5)	(6)	(7)	(8)	(9)	(10)	(11)	(12)	(13)
J0013093−002551	00 13 09.34	−00 25 51.5	1999.838	19.8	17.2	14.37	2.22	0.88	14.3	0.6	7.6	a
J0100021−615627	01 00 02.13	−61 56 27.1	1999.964	21.8	17.8	15.01	2.42	0.94	14.7	0.7	7.8	a
J0436278−411446	04 36 27.84	−41 14 46.9	1999.893	**	**	16.04	2.92	1.12	12.8	2.1	7.8	a
J0518113−310153	05 18 11.32	−31 01 53.0	2000.011	19.5	16.8	14.17	2.30	1.00	12.3	0.6	7.7	a
J1236396−172216	12 36 39.61	−17 22 16.9	1999.384	18.2	16.2	13.91	2.14	1.14	12.9	0.9	7.6	a
J1538317−103850	15 38 31.70	−10 38 50.6	2000.414	18.3	16.4	14.36	2.18	0.95	10.9	1.4	7.6	a
J1552237−033520	15 52 23.78	−03 35 20.7	1999.534	15.8	13.2	12.02	2.07	1.37	9.5	0.8	7.5	a
J1553186−025919	15 53 18.65	−02 59 19.3	1999.581	17.0	15.1	13.12	2.04	1.36	10.4	0.9	7.5	a
J2022480−564556	20 22 48.01	−56 45 56.8	2000.477	19.2	15.8	13.81	2.06	0.80	13.4	0.5	7.5	a
J2206227−204706*	22 06 22.78	−20 47 06.0	1999.611	20.1	17.9	15.09	2.67	1.22	14.1	1.4	7.9	a
J2226443−750342	22 26 44.36	−75 03 42.7	1999.814	21.5	18.3	15.20	2.84	1.20	13.7	1.1	7.9	a

* Previously listed by Gizis et al. (2000).
** Too faint for the plate.
Columns 1–4: DENIS name, position with respect to equinox J2000 at DENIS epoch, and DENIS epoch.
Columns 5, 6: B and *R* photographic magnitudes.
Columns 7–9: DENIS *I*-magnitude and colours.
Columns 10, 11: H_I *I*-band reduced proper, and its standard error.
Column 12: maximum RPM for a giant of the same $I-J$ colour.
Column 13: references for the proper motion and the *B* and *R* photometry: (a) our measurements; (b) *B* and *R* from the USNO-A2.0 catalogue (Monet et al. 1998) and proper motion from the UCAC1 catalogue (Zacharias et al. 2000); (c) *B* and *R* from the USNO-A2.0 catalogue (Monet et al. 1998) and proper motion from the Tycho-2 catalogue (Høg et al. 2000).

adopt 22 pc as the completeness limit of our sample, and use the 45 stars within that distance to determine the local density of late-M dwarfs. Using the Reid & Cruz (2002) ($I-J$, M_I) relation would give slightly larger distances and change the completeness distance to 25 pc.

A sample limited by photometric distance is effectively a magnitude-limited sample, with a colour-dependent magnitude limit. As such, and since the colour-luminosity relation has significant dispersion, it is subject to the well-know Malmquist bias (Malmquist 1936), through two separate but interrelated effects (e.g. Stobie et al. 1989 and Kroupa 1998):

- The average luminosity at a given colour is brighter for a magnitude-limited sample than for a volume-limited sample, since the brighter stars are included to larger distances, hence in larger numbers, than the fainter ones. This is the classical Malmquist bias;
- A magnitude-limited sample includes more stars at a given colour than the equivalent volume-limited sample for the average colour-luminosity relation: since the volume grows as d^3, the additional volume from which brighter stars get included is larger that the missing volume from which fainter stars are lost.

Here we are only interested in the colour-integrated stellar density over $2.0 \leq I-J \leq 3.0$ (or $11.9 \leq M_I \leq 14.0$). The first component of the Malmquist bias is therefore irrelevant, since a) we do not look for any significant luminosity resolution, and b) the luminosity function is sufficiently flat over the M 6–M 8 spectral range (Delfosse & Forveille 2000) that a small shift in the average luminosity will not measurably affect the resulting density. The second component of the bias, on the other hand, is significant. For a Gaussian dispersion of the colour-luminosity relation it can be computed analytically (Stobie et al. 1989):

$$\frac{\Delta\Phi}{\Phi} = \frac{1}{2}\sigma^2(0.6\ln 10)^2 \qquad (8)$$

where Φ is the luminosity function and σ is the intrinsic rms scatter in the colour-luminosity relation. The scatter in the M_I vs. $I-J$ relation is $\sigma \sim 0.2$ mag (Fig. 1), which corresponds to a 4% overestimate of the stellar density.

The mean surface density of our sample, 0.66 ± 0.11 objects per 100 square degrees out to 22 pc, corresponds to an uncorrected luminosity function of $\overline{\Phi}_I = (2.3 \pm 0.4) \times 10^{-3}$ stars M_I^{-1} pc^{-3}. After correcting for the Malmquist bias, this becomes $\overline{\Phi}_{I\,\mathrm{cor}} = (2.2 \pm 0.4) \times 10^{-3}$ stars M_I^{-1} pc^{-3}, averaged over $11.9 \leq M_I \leq 14.0$. Using relations from Leggett (1992) and Dahn et al. (2002) to translate to M_V, this gives $\overline{\Phi}_{V\,\mathrm{cor}} = (1.7 \pm 0.3) \times 10^{-3}$ stars M_V^{-1} pc^{-3}, averaged over $15.4 \leq M_V \leq 18.7$.

Stellar luminosity functions for the solar neighborhood come in two kinds: photometric luminosity functions, with

Table 4. Observational informations and Reduced Proper Motions for the 52 probable giants with $H_I - H_I^{\max} < 1\sigma$ in the full 5700 square degrees (same Cols. as Table 3c).

DENIS name	α_{2000}	δ_{2000}	DENIS epoch	B	R	I	$I-J$	$J-K$	H_I	err H_I	$H_I^{\max}$	Ref.
J0103401−854203	01 03 40.19	−85 42 03.7	1996.978	11.4	9.0	9.25	2.19	0.92	6.4	0.3	7.6	b
J0134067−101403[g]	01 34 06.71	−10 14 03.6	2000.660	13.3	10.9	11.38	2.01	1.14	4.7	2.3	7.5	b
J0136144−082710	01 36 14.44	−08 27 10.5	1999.940	18.4	15.1	14.01	2.47	1.16	9.1	2.4	7.8	a
J0250072−860930[g]	02 50 07.20	−86 09 30.0	1999.712	13.5	11.4	9.26	2.09	1.41	5.8	2.1	7.5	b
J0441247−271453	04 41 24.70	−27 14 53.6	1999.063	11.3	9.3	8.92	2.19	1.20	4.8	0.3	7.6	b
J0451504−750335[g]	04 51 50.48	−75 03 35.7	1998.816	15.0	13.8	13.69	2.14	2.42	12.1	1.1	7.6	a
J0457108−131240	04 57 10.85	−13 12 40.3	1996.060	14.1	13.2	10.57	2.16	1.26	5.6	2.8	7.6	a
J0504267−744821	05 04 26.74	−74 48 21.8	1996.964	19.3	16.0	13.79	2.11	1.36	5.5	32.6	7.6	a
J0538515−645534[g]	05 38 51.59	−64 55 34.4	1996.964	17.3	14.9	13.59	2.03	1.51	7.7	17.0	7.5	a
J0543339−782122	05 43 33.95	−78 21 22.4	1996.964	15.5	13.5	10.67	2.46	1.44	5.8	2.9	7.8	b
J0953338−014950	09 53 33.87	−01 49 50.2	2000.164	16.3	13.7	10.31	2.25	1.37	5.4	2.4	7.7	a
J1021323−204407	10 21 32.30	−20 44 07.4	2000.263	**	**	16.09	2.98	1.11	...	...	...	
J1034458−175302	10 34 45.89	−17 53 02.5	2000.197	16.8	14.3	12.01	2.64	1.26	8.7	1.3	7.9	b
J1125068+001513	11 25 06.87	+00 15 13.9	2000.268	15.4	13.3	10.60	2.32	1.24	4.6	4.0	7.7	a
J1221525−135310[g]	12 21 52.50	−13 53 10.3	1999.148	17.5	10.7	10.38	2.56	1.25	0.4	19.6	7.9	a
J1338300−294135	13 38 30.05	−29 41 35.2	2000.129	16.0	13.9	11.53	2.35	1.27	6.1	3.9	7.7	b
J1351326−291851	13 51 32.68	−29 18 51.9	2000.362	16.4	13.2	11.19	2.28	1.30	7.4	1.4	7.7	b
J1400335−271656	14 00 33.51	−27 16 56.2	1999.348	14.6	11.5	9.69	2.09	1.26	5.6	0.2	7.5	a
J1405376−221515	14 05 37.64	−22 15 15.0	1999.285	**	**	9.49	2.09	1.29	...	...	...	
J1409294−164227	14 09 29.49	−16 42 27.0	2000.510	15.5	13.5	10.46	2.24	1.29	4.3	2.2	7.7	b
J1427297−264040	14 27 29.71	−26 40 40.8	1999.419	15.9	10.8	9.68	2.12	1.20	5.5	1.8	7.6	b
J1437524−183824	14 37 52.45	−18 38 24.0	2000.414	14.2	12.0	12.86	2.10	0.92	8.3	2.1	7.5	b
J1503320−113217[g]	15 03 32.06	−11 32 17.3	2000.551	18.0	15.0	11.25	2.81	1.38	6.4	1.1	7.9	b
J1503339−185239	15 03 33.92	−18 52 39.1	2000.551	14.5	12.6	10.39	2.05	1.26	3.8	7.0	7.5	b
J1510397−212524	15 10 39.72	−21 25 24.9	1999.384	14.1	12.6	10.06	2.22	1.18	6.8	1.4	7.6	b
J1512333−103241	15 12 33.30	−10 32 41.3	2000.277	**	**	16.00	2.90	1.18	...	...	...	
J1525014−032359	15 25 01.46	−03 23 59.5	1999.351	14.1	11.6	9.25	2.09	1.08	5.0	0.8	7.5	c
J1539153+004404[g]	15 39 15.30	+00 44 04.0	2000.411	15.8	12.5	11.78	2.10	1.31	5.3	4.1	7.5	a
J1552551−045215	15 52 55.19	−04 52 15.3	1999.534	14.1	11.8	10.21	2.01	1.38	8.5	1.6	7.5	a
J1601227−093816	16 01 22.79	−09 38 16.2	2000.323	14.3	11.6	10.47	2.07	1.25	4.7	3.2	7.5	a
J1615446−040526	16 15 44.69	−04 05 26.2	1999.353	14.3	11.5	9.67	2.03	1.19	4.2	7.3	7.5	a
J1952020−553558	19 52 02.08	−55 35 58.8	2000.477	16.6	13.6	11.26	2.35	1.27	5.1	6.2	7.7	b
J2004401−395151	20 04 40.14	−39 51 51.7	2000.515	14.4	12.1	9.72	2.00	1.31	4.7	3.5	7.5	b
J2015585−712313	20 15 58.52	−71 23 13.2	2000.529	17.2	11.1	10.89	2.59	1.26	4.5	6.3	7.9	b
J2016341−772709	20 16 34.12	−77 27 09.4	2000.537	17.3	14.5	11.58	2.44	1.29	8.1	1.4	7.8	a
J2023115−283921	20 23 11.54	−28 39 21.5	2000.477	14.7	12.5	10.21	2.19	1.28	5.8	3.0	7.6	b
J2024329−294402[g]	20 24 32.96	−29 44 02.6	1999.392	14.8	14.3	10.45	2.13	1.26	6.0	3.0	7.6	b
J2032270−273058	20 32 27.03	−27 30 58.4	1999.534	15.0	12.3	10.76	2.45	1.18	7.6	2.4	7.8	a
J2036432−170727	20 36 43.24	−17 07 27.1	2000.592	14.9	11.5	9.40	2.00	1.24	4.6	1.0	7.5	b
J2044066−173457	20 44 06.68	−17 34 57.3	1999.606	16.1	13.3	11.28	2.42	1.29	5.5	5.2	7.8	b
J2055240−322600	20 55 24.07	−32 26 00.8	1999.669	14.4	13.4	10.73	2.10	1.30	8.1	1.0	7.5	b
J2056329−782540	20 56 32.90	−78 25 40.1	1999.660	15.5	12.4	10.43	2.08	1.20	7.9	1.3	7.5	b
J2058075−730350	20 58 07.55	−73 03 50.4	1999.660	17.6	14.1	11.89	2.35	1.29	6.5	6.6	7.7	a
J2103375−783831	21 03 37.56	−78 38 31.5	1999.658	16.2	13.9	11.42	2.08	1.30	4.8	8.1	7.5	b
J2107070−361729	21 07 07.01	−36 17 29.8	1996.422	15.9	13.0	11.61	2.09	1.30	6.8	3.4	7.5	b
J2108330−212051[g]	21 08 33.06	−21 20 51.3	2000.567	17.0	11.7	9.80	2.13	1.27	7.8	1.8	7.6	a
J2124575−341655	21 24 57.51	−34 16 55.9	1999.559	18.0	13.7	13.60	2.37	1.32	8.6	6.4	7.8	a
J2130021−815158	21 30 02.15	−81 51 58.6	1999.510	15.2	12.2	10.33	2.17	1.37	3.4	9.6	7.6	b
J2141290−844040	21 41 29.02	−84 40 40.1	2000.616	14.9	12.0	11.02	2.11	1.29	5.4	5.3	7.6	b
J2203522−593300	22 03 52.29	−59 33 00.7	1999.649	12.5	12.2	11.29	2.43	1.16	7.8	2.0	7.8	b
J2225004−121606	22 25 00.48	−12 16 06.9	1999.447	15.0	12.4	10.38	2.25	1.19	3.7	2.4	7.7	b
J2239371−715950	22 39 37.13	−71 59 50.0	2000.616	14.5	12.1	10.17	2.03	1.27	7.4	1.3	7.5	b

** Too faint for the plate.

[g] Previously known giants.

Table 5. a) Estimated distances and other parameters for the 24 high-PM of Tables 2a and 3a and 11 low-PM DENIS red dwarf candidates of Tables 2c and 3c.

DENIS objects	M_I	D [pc]	V_t [km s^{-1}]	T_{eff} [K]	Ref.	DENIS objects	M_I	D [pc]	V_t [km s^{-1}]	T_{eff} [K]	Ref.
J0013093−002551*	12.59	22.7	10.4	2630		J1141440−223215	13.56	23.6	47.4	2350	
J0020231−234605	12.99	21.4	33.4	2520		J1145354−202105	12.39	19.5	14.9	2670	
J0100021−615627*	13.05	24.6	10.3	2510		J1147421+001506	12.10	16.5	21.5	2740	a
J0103119−535143	12.72	23.1	26.1	2600		J1155429−222458	13.34	10.7	21.3	2420	
J0120491−074103	13.64	26.0	14.3	2320		J1201421−273746	12.57	22.2	36.2	2630	
J0144318−460432	12.51	20.8	12.5	2650		J1236396−172216*	12.36	20.4	6.0	2680	
J0218579−061749	13.45	26.4	47.4	2380	d	J1250526−212113	13.35	12.2	32.2	2410	
J0235495−071121	12.84	23.6	33.4	2570		J1538317−103850*	12.48	23.8	2.3	2650	
J0306115−364753	13.67	14.0	48.0	2310		J1552237−033520*	12.14	9.5	1.4	2730	
J0320588−552015	12.62	21.7	40.9	2620		J1553186−025919*	12.03	16.5	2.2	2750	
J0351000−005244	13.29	12.4	28.0	2430	a	J1610584−063132	12.17	18.1	16.0	2720	
J0436278−411446*	13.92	26.6	2.8	2250		J2022480−564556*	12.10	22.0	8.8	2740	
J0517377−334903	13.85	16.4	44.8	2270		J2132297−051158	12.30	17.5	29.4	2690	d
J0518113−310153*	12.80	18.8	3.7	2580		J2205357−110428	12.33	18.5	27.9	2690	b
J1006319−165326	13.09	19.6	34.0	2490	e	J2206227−204706*	13.48	21.0	6.4	2370	c
J1021513−032309	12.82	22.2	26.2	2570		J2226443−750342*	13.76	19.4	4.6	2290	
J1048126−112009	12.80	4.9	38.0	2580	a	J2337383−125027	12.33	18.5	32.7	2690	d
J1106569−124402	13.03	16.9	25.2	2510	b						

* Low-PM red dwarf candidates.
Column 1: object name.
Columns 2, 3: M_I absolute I-band magnitude and photometric distance.
Column 4: V_t tangential velocity. The small values (all below 55 km s^{-1}) point to a sample dominated by disk populations.
Column 5: T_{eff} effective temperature, derived from our ($I - J$, T_{eff}) calibration (see below).
Column 6: reference for a previously known trigonometric parallax: (a) Gliese & Jahreiß (1991) (CNS3 catalogue); for a spectrophotometric distance: (b) Kirkpatrick et al. (1997); (c) Gizis et al. (2000); (d) Cruz & Reid (2002); (e) McCaughrean et al. (2002); or for a photometric distance: (f) Reid & Cruz (2002).

somewhat uncertain distances and luminosities estimated from colour-luminosity relations, and nearby star luminosity functions, with distances (mostly) from trigonometric parallaxes but with typically smaller samples and sometimes an uncertain completeness. Figure 7 compares the above stellar density measurement with the photometric luminosity functions of Kroupa (1995a) and Zheng et al. (2001), as well as with the nearby star luminosity functions of Kroupa (1995a) and Reid et al. (2002). We measure the stellar density from a nearby sample, as the nearby luminosity functions do, but with the distance method from photometric luminosity functions. Our measurement is thus of interest to the long-standing discrepancy between the two measurement techniques. Our value of $\overline{\Phi}_{V\,\mathrm{cor}} = (1.7 \pm 0.3) \times 10^{-3}$ stars M_V^{-1} pc^{-3} turns out to be in excellent agreement with all recent measurements of the photometric luminosity function (e.g. Fig. 7 and caption). The nearby star luminosity function is, by contrast, over an order of magnitude larger. This clearly excludes that a local faint star overdensity can explain the discrepancy, as sometimes suggested in spite of serious kinematic difficulties. The true explanation most likely will have to be found in a bias of the photometric luminosity function methodology, such as the neglecting of unresolved binary systems (Kroupa 1995b), or potentially the use of an incorrect colour-luminosity relation (Reid & Gizis 1997; Delfosse & Forveille, in preparation). For a constant-density population, a systematic error in the stars luminosity function of Δm results in a luminosity function that is incorrect by:

$$\frac{\Delta\Phi}{\Phi} = 0.6 \ln 10 \Delta m \simeq 1.38 \Delta m. \quad (9)$$

In the ($I - J$) range of interest here, Fig. 1 shows that the dispersion of the calibration stars around our adopted relation is 0.25 mag. Similarly, the rms difference between our relation and that of Reid & Cruz (2002) is only 0.13 mag, and the maximum difference is below 0.2 mag. A 0.2 mag error on the color-luminosity relation is thus a conservative upper bound. This would affect the luminosity function at the 25–30% level at most, well below the difference between

Table 5. b) Estimated distances and other parameters for the 15 DENIS red dwarf candidates initially selected from NLTT of Tables 2b and 3b (same Cols. as Table 5a).

DENIS objects	M_I	D [pc]	V_t [km s^{-1}]	$T_{\rm eff}$ [K]	Ref.
J0002061+011536	13.25	20.4	46.3	2440	
J0410480−125142	12.07	15.3	29.0	2740	d
J0440231−053009	13.39	9.8	15.3	2400	d, e
J0520293−231848	12.72	18.2	28.8	2600	
J0931223−171742	12.84	12.7	19.0	2570	
J1346460−314925	12.65	13.3	23.5	2620	
J1504161−235556	13.53	17.3	26.7	2360	f
J1546115−251405	12.20	23.8	42.8	2710	
J1552446−262313	12.65	9.8	24.4	2620	
J1553571−231152	12.07	20.6	29.6	2740	f
J1625503−240008	12.97	19.2	14.7	2530	
J1641430−235948	12.39	22.3	22.8	2670	
J1645282−011228	12.36	24.2	25.2	2680	
J1917045−301920	12.27	20.3	27.0	2700	
J2151270−012713	11.96	17.8	18.6	2760	d

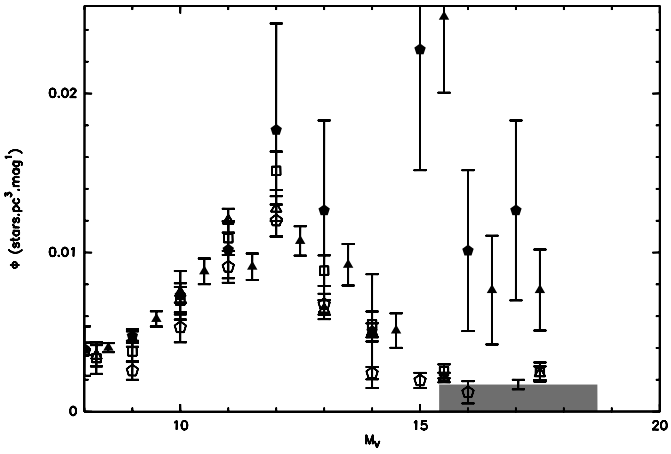

Fig. 7. The M_V luminosity function. Open symbols are photometric luminosity function (triangles and squares are two Galactic models from Zheng et al. 2001; polygons are from Kroupa 1995a). Filled symbol represent nearby star luminosity functions (triangles from Reid et al. 2002, and polygons from Kroupa 1995a). The filled grey area shows our stellar density estimate for M 6 to M 8 stars, which is in excellent agreement with other photometric luminosity functions.

photometric and nearby stars luminosity functions. We obtain a more realistic estimate of the probable star density error stemming from colour-luminosity uncertainties by using the Reid & Cruz (2002) calibration (Fig. 1) instead of our own. The completeness limit is then 25 pc, with 51 stars within that distance, for a luminosity function of $\overline{\Phi}_{V\,\rm cor} = (1.55 \pm 0.3) \times 10^{-3}$ stars M_V^{-1} pc^{-3}. This is just ∼10% smaller than our best estimate, and actually well below its Poisson probable error.

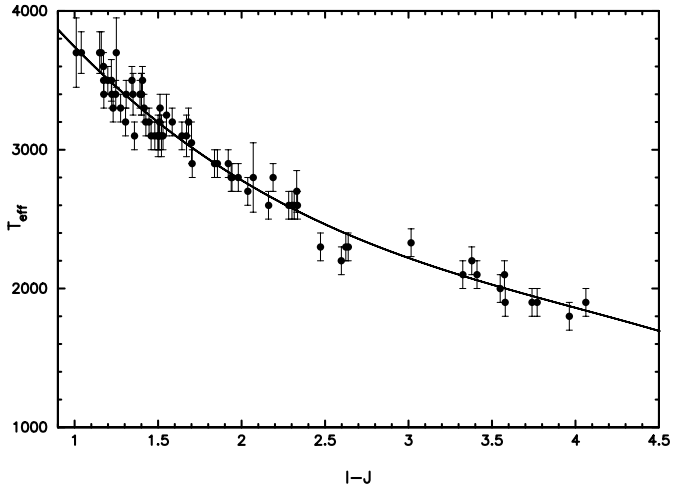

Fig. 8. The polynomial ($I-J$, $T_{\rm eff}$) relation, fitted to data from Leggett, Basri et al., Tinney et al., and Bessell, see text.

Since parallaxes out to 30 pc can be measured very accurately (Dahn et al. 2002; Henry et al. 1997), though certainly with significant efforts, true distances could be measured for the present well understood sample, and would certainly help clarifying the source of this discrepancy.

7. Effective temperature

The effective temperature $T_{\rm eff}$ of a star is one of its basic physical parameters, and we felt that a convenient rough estimate would be useful. We compiled the data from Leggett et al. (1996, 2000, 2001); Basri et al. (2000); Tinney et al. (1993), Bessell (1991), transformed when necessary to the CIT system with the relations from Leggett (1992) and Casali & Hawarden 1992), and adjusted the following cubic relation (Fig. 8):

$$T_{\rm eff} = b_0 + b_1(I-J) + b_2(I-J)^2 + b_3(I-J)^3 \qquad (10)$$

where $b_0 = 5297.3$, $b_1 = -1926.3$, $b_2 = 400.0$, $b_3 = -33.3$ valid for $1.0 \le I - J \le 4.1$.

It strictly speaking is only valid for CIT photometry, but Fig. 1 shows that the DENIS and CIT systems are sufficiently close that it provides an acceptable determination of $T_{\rm eff}$ from DENIS photometry.

Tables 5a and 5b lists the effective temperatures derived from the DENIS $I-J$ colour index with this formula.

8. Future prospects

Compared with the cruder proper motion cutoff, selection on reduced proper motion contributes 11 additional probable dwarfs in a sample of 62. This 18% fraction, which may be a lower limit if a few additional dwarfs hide amongst the probable giants, is much larger than the 6% loss estimated in Paper I.

It is therefore important to obtain spectroscopy to make sure that all 11 low-PM dwarf candidates are really dwarfs, and to determine which, if any, of the 52 probable giants are actually very low tangential velocity dwarfs. We additionally plan

Table 6. Comparison between our photometric distances from ($I - J$, M_I) and literature distances, based on either trigonometric parallaxes or spectrophotometric distances with stated accuracies better than 4 pc. The Hipparcos distance quoted for LP 793-34 results from the parallax of its common proper motion companion, LP 793-33.

DENIS name	Other name	Our distance [pc]	Previous distance [pc]	Source
J0351000−005244	GJ 3252	12.4	14.7 ± 0.4	Gliese & Jahreiß (1991)
J0410480−125142	LP 714-37	15.3	19.4 ± 2.1	Cruz & Reid (2002)
J0440231−053009	LP 655-48	9.8	8.0 ± 1.6	McCaughrean et al. (2002)
		9.8	15.3 ± 2.6	Cruz & Reid (2002)
J1048126−112009	GJ 3622	4.9	4.5 ± 0.1	Gliese & Jahreiß (1991)
J1106569−124402	LP 731-47	16.9	$18.0\ ^{+3}_{-2}$	Kirkpatrick et al. (1997)
J1145354−202105	LP 793-34	19.5	20.2 ± 1.5	Hipparcos, for LP 793-33
J1147421+001506	GJ 3686B	16.5	15.6 ± 2.9	Gliese & Jahreiß (1991)
J2132297−051158	LP 698-2	17.5	23.7 ± 2.8	Cruz & Reid (2002)
J2151270−012713	LP 638-50	17.8	21.0 ± 1.5	Cruz & Reid (2002)
J2337383−125027	LP 763-3	18.5	21.5 ± 2.3	Cruz & Reid (2002)

to extend the systematic search to the rest of the DENIS data, as they become available, as well as to the much more numerous early M-dwarfs candidates ($1 \leq I - J < 2$, M 0–M 6). A larger fraction of those is probably already known however.

Acknowledgements. We are grateful to René Chesnel for scanning and pre-reducing the photographic plates. The long-term loan of POSS I plates by the Leiden Observatory to Observatoire de Paris is gratefully acknowledged. This research has made an intensive use of the Simbad and Vizier databases, operated at CDS, Strasbourg, France. We thank the referee for many valuable comments and suggestions.

References

Arenou, F., & Luri, X. 1999, in Harmonizing Cosmic Distance scales in a Post-Hipparcos Era, ed. D. Egret, & A. Heck, ASP Conf. Ser., 107, 13
Baraffe, I., Chabrier, G., Allard, F., & Hauschildt, P. H. 1998, A&A, 337, 403
Basri, G., Mohanty, S., Allard, F., et al. 2000, ApJ, 538, 363
Berger, J., Cordoni, J.-P., Fringant, A.-M., et al. 1991, A&AS, 87, 389
Bertin, E., & Arnouts, S. 1996, A&AS, 117, 393
Bessell, M. S., & Brett, J. M. 1988, PASP, 100, 1134
Bessell, M. S. 1991, AJ, 101, 662
Bucciarelli, B., García Yus, J., Casalegno, R., et al. 2001, A&A, 368, 335
Casali, M., & Hawarden, T. G. 1992, UKIRT Newsletter, 4, 33
Cruz, K. L., & Reid, I. N. 2002, AJ, 123, 2828
Dahn, C. C., Harris, H. C., Vrba, F. J., et al. 2002, AJ, 124, 1170
Deacon, N. R., & Hambly, N. C. 2001, A&A, 380, 148
Dehnen, W., & Binney, J. J. 1998, MNRAS, 298, 387
Delfosse, X. 1997b, Ph.D. Thesis, Fig. 2.9, Grenoble University, 43
Delfosse, X., Forveille, T., Beuzit, J. L., et al. 1999, A&A, 344, 897
Delfosse, X., & Forveille, T. 2000, in Very Low-mass Stars and Brown Dwarfs, ed. R. Rebolo, & M. R. Zapatero-Osorio (Cambridge: Cambridge University Press), 84
Delfosse, X., & Forveille, T. 2001, in SF2A-2001, EDP Sciences, Conf. Ser., 91
Epchtein, N. 1997, in the 2nd DENIS Euroconference, The impact of large scale near-infrared surveys, ed. F. Garzon et al. (Dordrecht: Kluwer), 15
ESA 1997, The Hipparcos and Tycho Catalogues, ESA SP-1200
Gizis, J. E., Monet, D. G., Reid, I. N., et al. 2000, AJ, 120, 1085
Gliese, W., Jahreiß, H., & Upgren, A. R. 1986, in The galaxy and the solar system, ed. R. Schmoluchowski, J. N. Bahcall, & M. S. Matthews (The University of Arizona Press), 13
Gliese, W., & Jahreiß, H. 1991, Preliminary Version of the Third Catalogue of Nearby Stars, as available at CDS Strasbourg
Hawley, S. L., Covey, K. R., Knapp, G. R., et al. 2002, AJ, 123, 3409
Henry, T. J., Ianna, P. A., Kirkpatrick, J. D., & Jahreiss, H., AJ, 114, 388
Henry, T. J., Walkowicz, L. M., Barto, T. C., & Golimowski, D. A. 2002, AJ, 123, 2002
Høg, E., Fabricius, C., Makarov, V. V., et al. 2000, A&A, 355, L27
Kerr, F. J., & Lynden-Bell, D. 1986, MNRAS, 221, 1023
Kirkpatrick, J. D., Henry, T. J., & Irwin, M. J. 1997, AJ, 113, 1421
Kirkpatrick, J. D., Reid, I. N., Liebert, J., et al. 1999, ApJ, 519, 802
Kroupa, P. 1995a, ApJ, 453, 350
Kroupa, P. 1995b, ApJ, 453, 358
Kroupa, P. 1998, in Brown Dwarf and Extrasolar Planets Workshop, ed. Rebolo, Martín, Zapatero Osorio, ASP Conf. Ser., 134, 483
Leggett, S. K. 1992, ApJS, 82, 531
Leggett, S. K., Allard, F., Berriman, G., Dahn, C. C., & Hauschildt, P. H. 1996, ApJS, 104, 117
Leggett, S. K., Allard, F., Dahn, C. C., et al. 2000, ApJ, 535, 965
Leggett, S. K., Allard, F., Geballe, T. R., Hauschildt, P. H., & Schweitzer, A. 2001, ApJ, 548, 908
Leonard, P. J. T., & Tremaine, S. 1990, AJ, 353, 486
Luyten, W. J. 1979, Catalogue of stars with proper motions exceeding 0.″5 annually (LHS) (Minneapolis: University of Minnesota)
Luyten, W. J. 1980, New Luyten catalog of stars with proper motions larger than Two Tenths of an arcsecond (NLTT) (Minneapolis: University of Minnesota)
Malmquist K. G. 1936, Stockholm Obs. Medd. 26
Martín, E. L., Basri, G., Delfosse, X., & Forveille, T. 1997, A&A, 327, L29
McCaughrean, M. J., Scholz, R.-D., & Lodieu, N. 2002, A&A, 390, L27

Meillon, L. 1999, Ap&SS, 265, 179
Monet, D., Bird, A., Canzian, B., et al. 1998, USNO-A2.0 Catalogue, available on-line in Vizier (CDS, Strasbourg)
Phan-Bao, N., Guibert, J., Crifo, F., et al. 2001, A&A, 380, 590
Postman, M., Bucciarelli, B., Sturch, C., et al. 1997, IAU Symp., 179, 379
Reid, I. N., & Gizis, J. E. 1997, AJ, 113, 2246
Reid, I. N., & Cruz, K. L. 2002, AJ, 123, 2806
Reid, I. N., Gizis, J. E., & Hawley, S. L. 2002, AJ, 124, 2721
Scholz, R.-D., Irwin, M., Ibata, R., Jahreiß, H., & Malkov, O. Yu. 2000, A&A, 353, 958
Scholz, R.-D., Meusinger, H., & Jahreiß, H. 2001, A&A, 374, L12
Skrutskie, M. F., Forrest, W. J., & Shure, M. 1989, AJ, 98, 1409
Skrutskie, M. F., Schneider, S. E., Stiening, R., et al. 1997, in the 2nd DENIS Euroconference, The impact of large scale near-infrared surveys, ed. F. Garzon et al. (Dordrecht: Kluwer), 25
Stobie, R. S., Ishida, K., & Peacock, J. A. 1989, MNRAS, 238, 709
Thé, P. S., Thomas, D., Christensen, C. G., & Westerlund, B. E. 1990, PASP, 102, 565
Tinney, C. G., Mould, J. R., & Reid, I. N. 1993, AJ, 105, 1045
Tinney, C. G., Reid, I. N., Gizis, J., & Mould, J. R. 1995, AJ, 110, 3014
Tinney, C. G. 1996, MNRAS, 281, 644
Urban, S. E., Corbin, T. E., & Wycoff, G. L. 1998, AJ, 115, 2161
van Altena, W. F., Lee, J. T., & Hoffleit, E. D. 1995, The General Catalogue of Trigonometric Stellar Parallaxes, Fourth Edition (New Haven, CT: Yale University Observatory)
York, D. G., Adelman, J., & Anderson, J. E. Jr. 2000, AJ, 120, 1579
Zacharias, N., Urban, S. E., Zacharias, M. I., et al. 2000, AJ, 120, 2131
Zheng, Z., Flynn, C., Gould, A., Bahcall, J. N., & Salim, S. 2001, ApJ, 555, 393